Supporting Information

Synthesis and Reactivity of *ortho*-Phosphane Oxide-Substituted Aryl(hydro)borates and Aryl(hydro)boranes.

Jens Michael Breunig, Felix Lehmann, Michael Bolte, Hans-Wolfram Lerner,
and Matthias Wagner*

Content:

1. NMR data/syntheses of Li[2a], 2b, Mg[5]$_2$, 9, 10, and (2-Br-C_6H_4)$Ph_2P\cdot B(H)(C_6F_5)_2$.

General Considerations: See the main paper.

NMR Data of Li[2a]. ^{1}H NMR (300.0 MHz, C_6D_6): δ = 1.20 (d, $^3J_{H,P}$ = 13 Hz, 18H; CCH_3), 3.26 (s, 6H; OCH_3), 3.71 (s, 3H; OCH_3), 7.03-7.09 (m, 1H; ArH), 7.33-7.40 (m, 1H; ArH), 7.42-7.48 (m, 1H; ArH), 9.16-9.20 (m, 1H; ArH); ^{11}B{^{1}H} NMR (96.3 MHz, C_6D_6): δ = 4.3 ($h_{1/2}$ = 60 Hz); ^{31}P{^{1}H} NMR (121.5 MHz, C_6D_6): δ = 67.4 ($h_{1/2}$ = 30 Hz).

NMR Data of 2b. ^{1}H NMR (300.0 MHz, C_6D_6): δ = 1.02 (d, $^3J_{H,P}$ = 15 Hz, 18H; CCH_3), 3.84 (s, 6H; OCH_3), 7.01-7.07 (m, 1H; ArH), 7.09-7.14 (m, 1H; ArH), 7.25-7.31 (m, 1H; ArH), 7.92-7.94 (m, 1H; ArH); ^{11}B{^{1}H} NMR (96.3 MHz, C_6D_6): δ = 15.5 ($h_{1/2}$ = 130 Hz); ^{31}P{^{1}H} NMR (121.5 MHz, C_6D_6): δ = 74.1 ($h_{1/2}$ = 18 Hz).

NMR data of Mg[5]$_2$. The NMR spectra of this compound are provided here to allow an in situ reaction control during the one-pot synthesis of **6**. Pure bulk material of [**5**]$^-$ is usually not accessible on a preparative scale, however, the purity is sufficient for further transformation into **6**. The NMR data given here were obtained on a number of manually selected single crystals of Mg(Et_2O)[**5**]$_2$×Et_2O.
^{1}H NMR (300.0 MHz, C_6D_6): δ = 0.95 (d, $^3J_{H,P}$ = 14 Hz, 18H; CCH_3), 1.06 (t, $^3J_{H,H}$ = 7 Hz, 6H; CH_2CH_3), 2.83 (q, $^1J_{H,B}$ = 74 Hz, 2H; BH), 3.41 (q, $^3J_{H,H}$ = 7 Hz, 4H; CH_2CH_3), 6.86-6.93 (m, 1H; ArH), 7.11-7.20 (m, 2H; ArH), 7.34 (br, 1H; ArH); ^{11}B NMR (96.3 MHz, C_6D_6): δ = –24.1 (t, $^1J_{H,B}$ = 74 Hz); ^{11}B{^{1}H} NMR (96.3 MHz, C_6D_6): δ = –24.1 ($h_{1/2}$ = 24 Hz); ^{31}P{^{1}H} NMR (121.5 MHz, C_6D_6): δ = 68.9 ($h_{1/2}$ = 23 Hz); ^{19}F NMR (282.3 MHz, C_6D_6): δ = –165.0 (m, 2F; F-*m*), –160.9 (m, 1F; F-*p*), –132.3 (m, 2F; F-*o*) [$\Delta\delta^{19}F_{m,p}$ = 4.1]; ^{13}C{^{1}H} NMR (75.4 MHz, C_6D_6): δ = 14.9 (s; CH_2CH_3), 26.8 (d, $^2J_{C,P}$ = 1 Hz; CCH_3), 37.0 (d, $^1J_{C,P}$ = 59 Hz; CCH_3), 65.2 (s; CH_2CH_3), 123.5 (d, $J_{C,P}$ = 13 Hz; ArC), 128.5 (d**; PC), 130.6 (d, $J_{C,P}$ = 17 Hz; ArC), 131.2 (s; ArC), 136.5 (d, $J_{C,P}$ = 14 Hz; ArC), 157.5 (BC)*, n.o. (FC). *) This signal was only observed in the 2D HMBC NMR experiment. **) Half of the doublet is hidden underneath the solvent resonance.

Synthesis of 9. An NMR tube was charged with $(C_6F_5)_2BH\cdot SMe_2$ (15 mg, 0.037 mmol) and *t*-$Bu_2P(O)Ph$, **1**, (9 mg, 0.04 mmol), the solid mixture was dissolved in C_6D_6 (0.5 mL), and investigated by NMR spectroscopy. X-ray quality crystals of **9** grew upon slow evaporation of the C_6D_6 under inert conditions.

^{1}H NMR (500.2 MHz, C_6D_6): δ = 0.87 (d, $^3J_{H,P}$ = 15 Hz, 18H; CCH_3), 4.91 (br, 1H; BH), 6.95-7.03 (m, 3H; PhH), 7.55-7.58 (m, 2H; PhH); ^{11}B NMR (160.5 MHz, C_6D_6): δ = –5.0 (n.r., $h_{1/2}$ = 370 Hz); ^{11}B{^{1}H} NMR (160.5 MHz, C_6D_6): δ = –5.0 ($h_{1/2}$ = 350 Hz); ^{31}P{^{1}H} NMR (202.5 MHz, C_6D_6): δ = 74.6 ($h_{1/2}$ = 18 Hz); ^{19}F NMR (470.6 MHz, C_6D_6): δ = –164.2 (m, 4F; F-*m*), –159.2 (m, 2F; F-*p*), –133.3 (m, 4F; F-*o*) [$\Delta\delta^{19}F_{m,p}$ = 5.0]; ^{13}C{^{1}H} NMR (125.8 MHz, C_6D_6): δ = 26.5 (d, $^2J_{C,P}$ = 1 Hz; C*C*H$_3$), 37.1 (d, $^1J_{C,P}$ = 55 Hz; *C*CH$_3$), 124.1 (d, $^1J_{C,P}$ = 86 Hz; PC), 128.7 (d, $J_{C,P}$ = 11 Hz; PhC), 132.5 (d, $J_{C,P}$ = 9 Hz; PhC), 133.1 (d, $^4J_{C,P}$ = 3 Hz; PhC-*p*), n.o. (BC), n.o. (FC).

Synthesis of 10. An NMR tube was charged with $(C_6F_5)_3B$ (50 mg, 0.098 mmol) and *t*-$Bu_2P(O)Ph$, **1**, (23 mg, 0.097 mmol), the solid mixture was dissolved in C_6D_6 (0.5 mL), and investigated by NMR spectroscopy.

^{1}H NMR (300.0 MHz, C_6D_6): δ = 0.81 (d, $^3J_{H,P}$ = 16 Hz, 18H; CCH_3), 6.83-6.92 (m, 2H; PhH), 6.98-7.03 (m, 1H; PhH-*p*), 7.31-7.37 (m, 2H; PhH); ^{11}B{^{1}H} NMR (96.3 MHz, C_6D_6): δ = 0.7 ($h_{1/2}$ = 580 Hz); ^{31}P{^{1}H} NMR (121.5 MHz, C_6D_6): δ = 77.7 ($h_{1/2}$ = 82 Hz); ^{19}F NMR (282.3 MHz, C_6D_6): δ = –164.3 (m, 6F; F-*m*), –157.3 (m, 3F; F-*p*), –129.0 (m, 6F; F-*o*) [$\Delta\delta^{19}F_{m,p}$ = 7.0].

Synthesis of (2-Br-C_6H_4)$Ph_2P\cdot B(H)(C_6F_5)_2$. $(C_6F_5)_2BH\cdot SMe_2$ (0.286 g, 0.701 mmol) and (2-Br-C_6H_4)PPh_2, **11**, (0.24 g, 0.70 mmol) were dissolved in toluene (15 mL) and the resulting reaction mixture was stirred for 2 d at room temperature. To remove SMe_2, the sample was evaporated to dryness under vacuum. The solid residue was redissolved in toluene (2.5 mL) and stored at –40 °C for 2 d to grow crystals suitable for X-ray diffraction. Yield: 263 mg (55%).

^{1}H NMR (500.2 MHz, C_6D_6): δ = 4.80 (br, 1H; BH), 6.55-6.58 (m, 1H; C_6H_4), 6.71-6.74 (m, 1H; C_6H_4), 6.87-6.90 (m, 4H; PhH), 6.91-6.93 (m, 1H; C_6H_4), 6.95-6.98 (m, 2H; PhH), 7.51-7.55 (m, 4H; PhH), 7.63-7.68 (m, 1H; C_6H_4); ^{11}B NMR (160.5 MHz, C_6D_6): δ = –22.1 (n.r., $h_{1/2}$ = 320 Hz); ^{11}B{^{1}H} NMR (160.5 MHz, C_6D_6): δ = –22.1 ($h_{1/2}$ = 245 Hz); ^{31}P{^{1}H} NMR (202.5 MHz, C_6D_6): δ = 18.4 ($h_{1/2}$ = 131 Hz); ^{19}F NMR (470.6 MHz, C_6D_6): δ = –164.2 (m,

4F; F-*m*), –157.7 (m, 2F; F-*p*), –127.6 (m, 4F; F-*o*) [$\Delta\delta^{19}F_{m,p}$ = 6.5]; $^{13}C\{^{1}H\}$ NMR (125.8 MHz, C_6D_6): δ = 124.5 (d, $^{1}J_{C,P}$ = 61 Hz; PC(Ph)), 127.4 (d, $J_{C,P}$ = 10 Hz; C_6H_4), 128.6 (d, $J_{C,P}$ = 13 Hz; BrC), 128.9 (d, $J_{C,P}$ = 11 Hz; PhC), 131.9 (d, $^{4}J_{C,P}$ = 3 Hz; PhC-*p*), 133.5 (d, $J_{C,P}$ = 2 Hz; C_6H_4), 134.2 (d, $J_{C,P}$ = 8 Hz; PhC), 135.2 (d, $J_{C,P}$ = 6 Hz; C_6H_4), 136.6 (d, $J_{C,P}$ = 10 Hz; C_6H_4), n.o. (PC(C_6H_4))*, n.o. (BC), n.o. (FC). *) According to a HMBC Experiment this signal is hidden underneath the solvent resonance.

2. ^{1}H and ^{13}C{^{1}H} NMR spectra of Li[3], Mg[5]$_2$, and Li[13]. ^{11}B and ^{31}P{^{1}H} NMR spectra of Li[3] and Li[13].

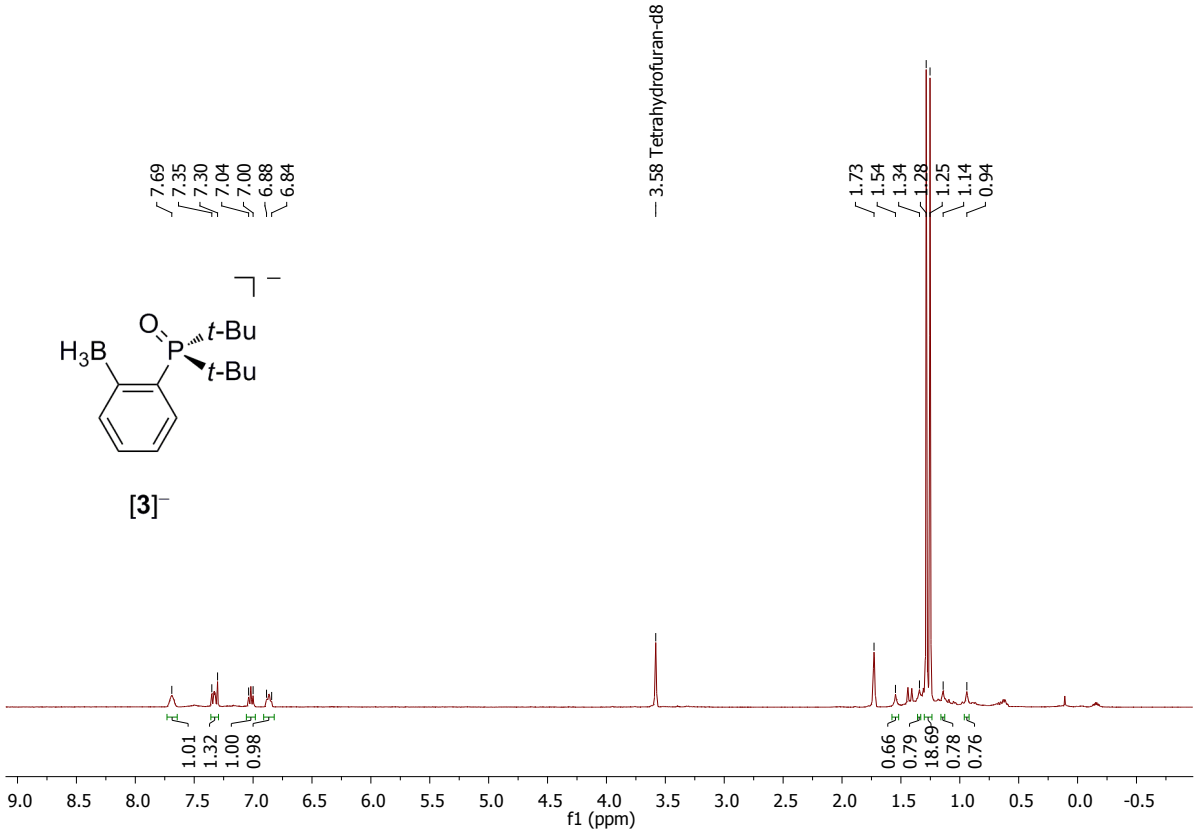

Figure S1. ^{1}H NMR spectrum of Li[**3**] (400.1 MHz, THF-d_8).

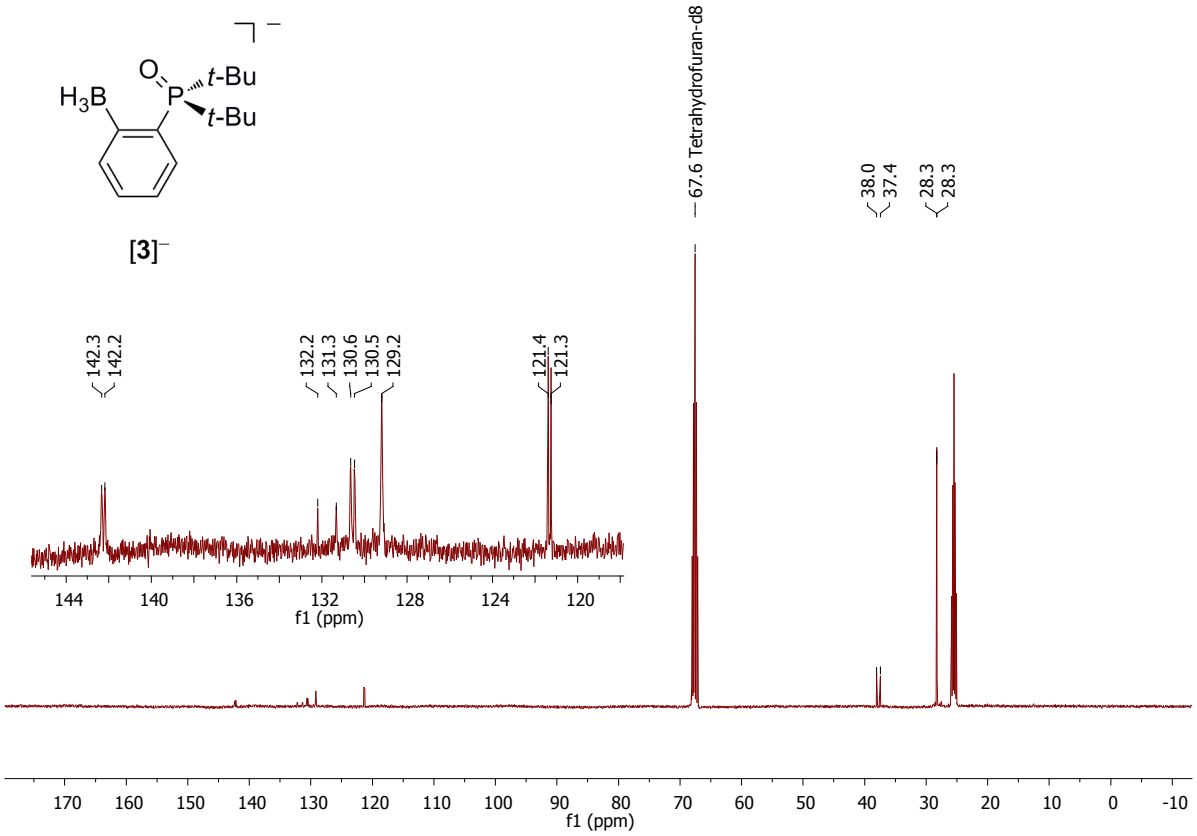

Figure S2. ^{13}C{^{1}H} NMR spectrum of Li[**3**] (100.6 MHz, THF-d_8).

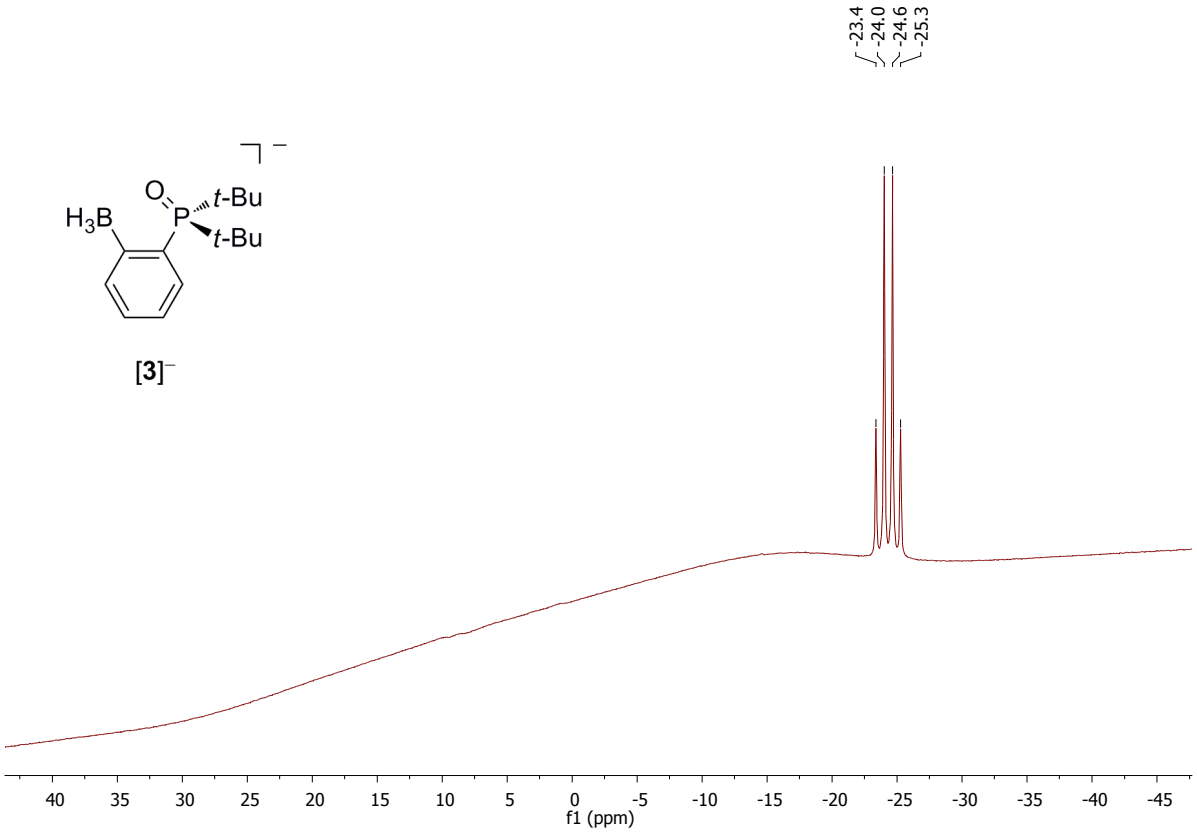

Figure S3. ^{11}B NMR spectrum of Li[**3**] (128.4 MHz, THF-d_8).

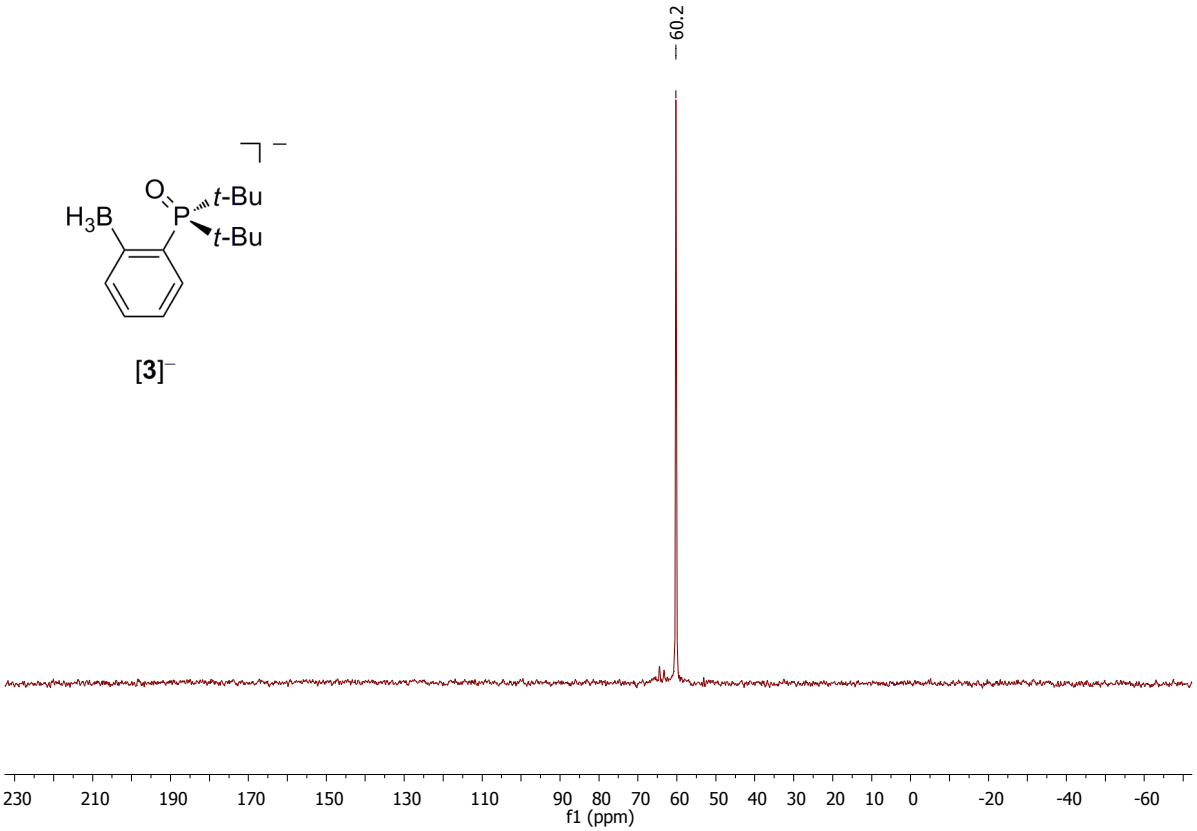

Figure S4. ^{31}P{^{1}H} NMR spectrum of Li[**3**] (162.0 MHz, THF-d_8).

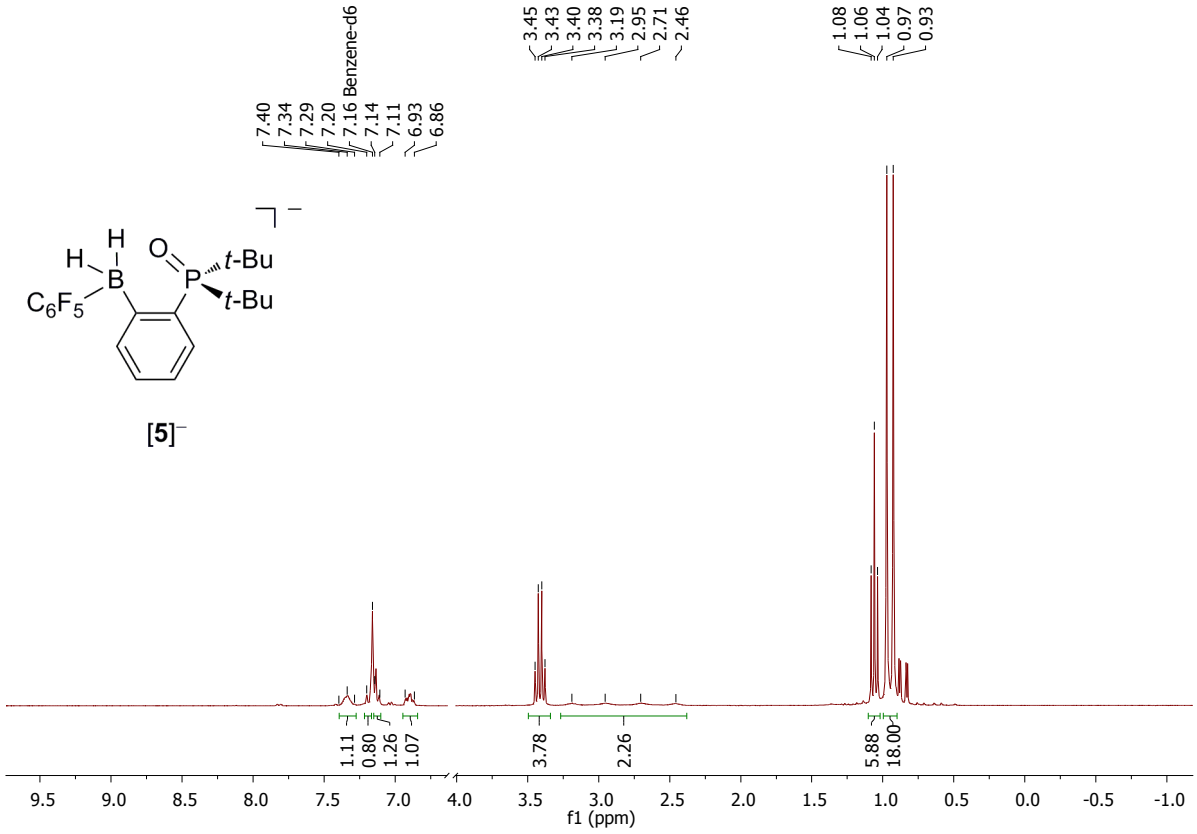

Figure S5. ^{1}H NMR spectrum of Mg[**5**]$_2$ (300.0 MHz, C_6D_6).

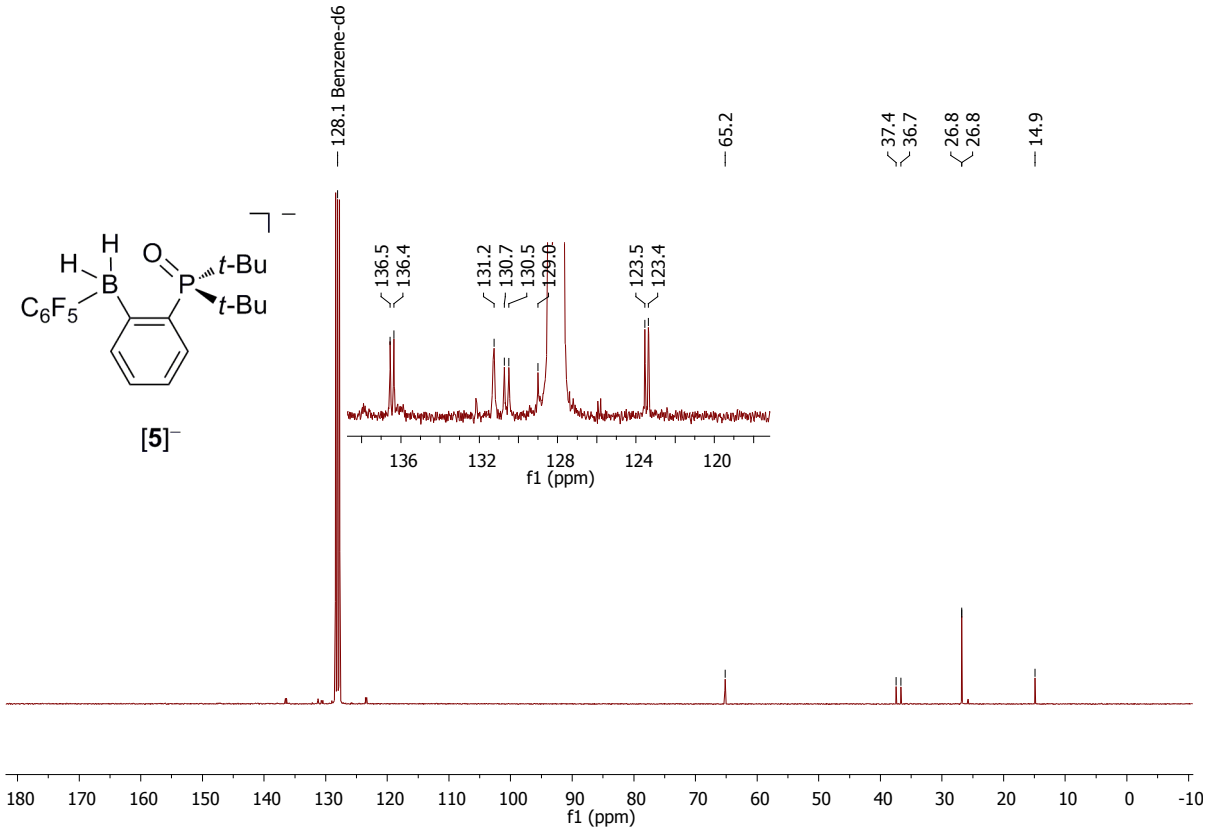

Figure S6. ^{13}C{^{1}H} NMR spectrum of Mg[**5**]$_2$ (75.4 MHz, C_6D_6).

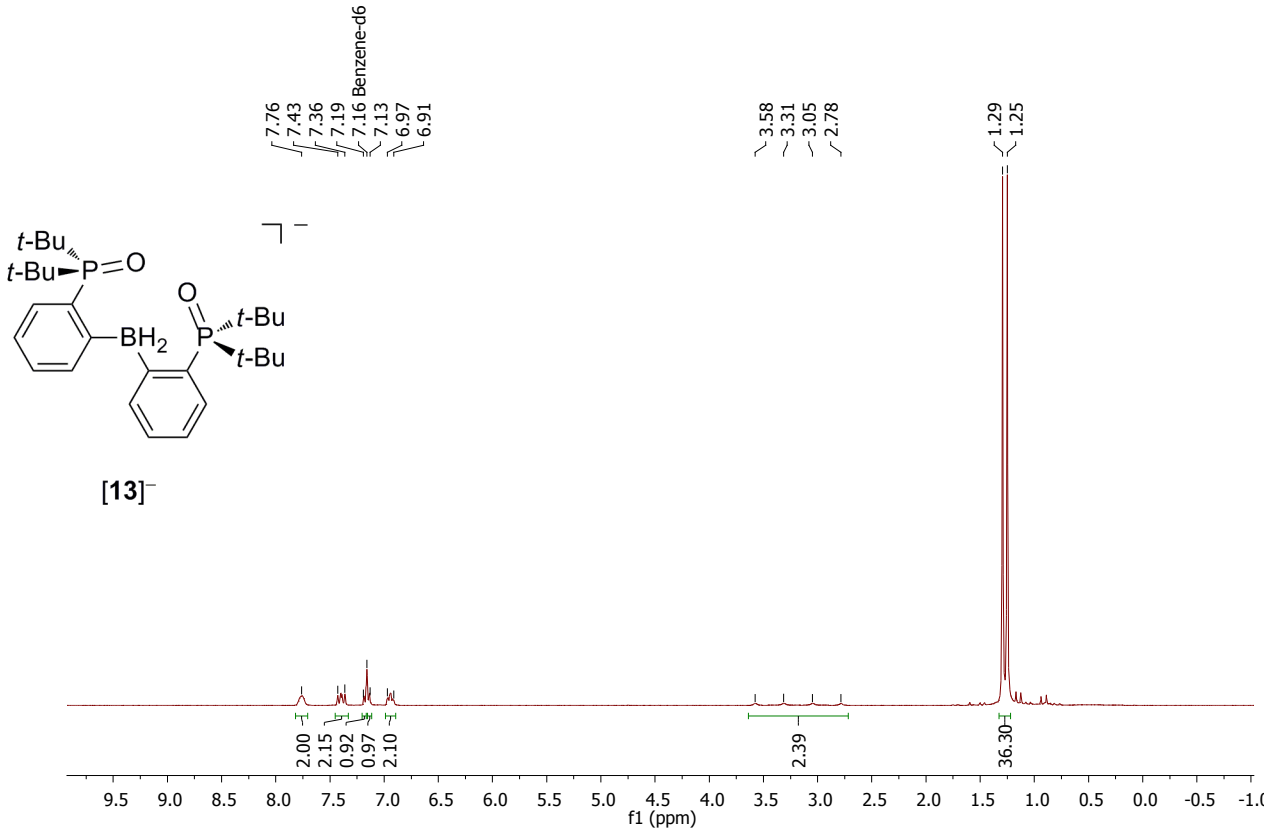

Figure S7. ^{1}H NMR spectrum of Li[**13**] (300.0 MHz, C_6D_6).

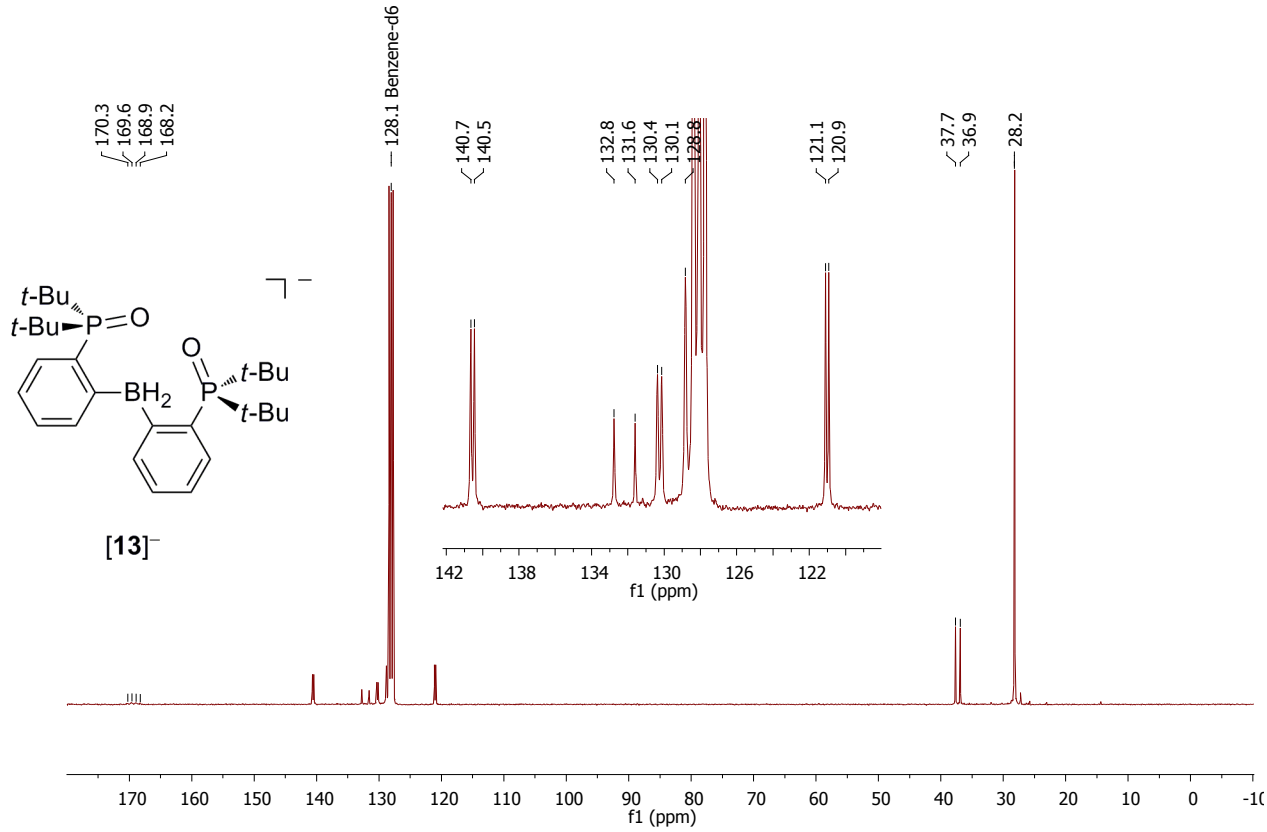

Figure S8. ^{13}C{^{1}H} NMR spectrum of Li[**13**] (75.4 MHz, C_6D_6).

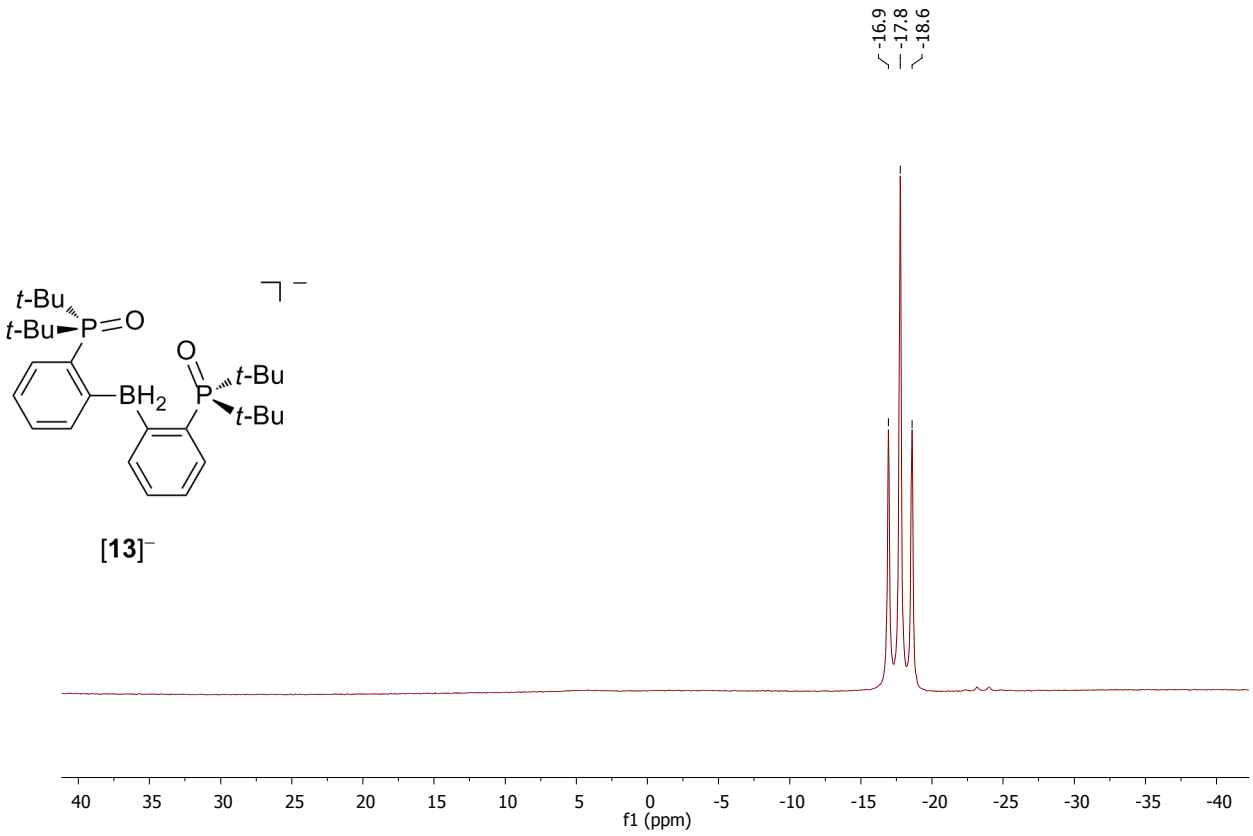

Figure S9. ^{11}B NMR spectrum of Li[**13**] (96.3 MHz, C_6D_6).

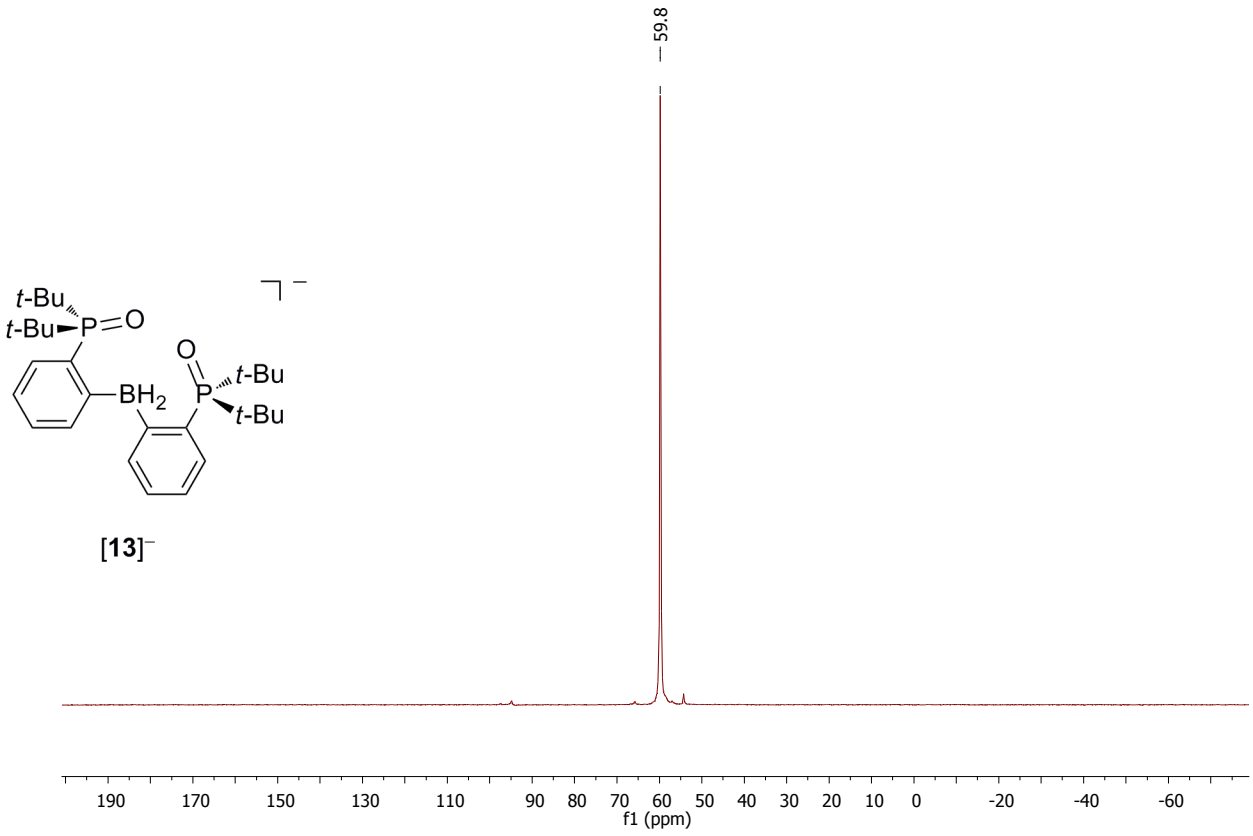

Figure S10. ^{31}P{^{1}H} NMR spectrum of Li[**13**] (121.5 MHz, C_6D_6).

3. X-ray crystal structure analyses of $(Li[2a])_2$, $(Li[3])_2 \times C_6H_6$, $(Li[3])_2$, 4, $Mg(Et_2O)[5]_2 \times Et_2O$, $Mg(Et_2O)[5]_2 \times 1.5\ Et_2O$, 6, 6*, $Mg[7]_2 \times 2\ C_6H_6$, $8 \times 0.5\ C_6H_6$, 9, 12, $(2\text{-}Br\text{-}C_6H_4)Ph_2P \cdot B(H)(C_6F_5)_2 \times 0.5$ toluene, $(Li[13])_2$, 1,2-$C_6H_4(P(O)t\text{-}Bu_2)(I)$, and 1,2-$C_6H_4(Pt\text{-}Bu_2)(Br)$.

X-ray Crystallographic Data. Data for **12** were collected on a STOE IPDS II two-circle diffractometer with graphite-monochromated MoK_α radiation (λ = 0.71073 Å) and corrected for absorption by an empirical absorption correction with the program *PLATON*[S1]. Data for $(Li[\mathbf{2a}])_2$, $(Li[\mathbf{3}])_2 \times C_6H_6$, $(Li[\mathbf{3}])_2$, **4**, $Mg(Et_2O)[\mathbf{5}]_2 \times Et_2O$, $Mg(Et_2O)[\mathbf{5}]_2 \times 1.5\ Et_2O$, **6**, **6***, $Mg[\mathbf{7}]_2 \times 2\ C_6H_6$, **8**$\times 0.5\ C_6H_6$, **9**, $(2\text{-}Br\text{-}C_6H_4)Ph_2P \cdot B(H)(C_6F_5)_2 \times 0.5$ toluene, $(Li[\mathbf{13}])_2$, 1,2-$C_6H_4(P(O)t\text{-}Bu_2)(I)$, and 1,2-$C_6H_4(Pt\text{-}Bu_2)(Br)$ were collected on a STOE IPDS II two-circle diffractometer with a Genix Microfocus tube with mirror optics also using MoK_α radiation. The data for $(Li[\mathbf{2a}])_2$, $(Li[\mathbf{3}])_2 \times C_6H_6$, $(Li[\mathbf{3}])_2$, **4**, $Mg(Et_2O)[\mathbf{5}]_2 \times Et_2O$, $Mg(Et_2O)[\mathbf{5}]_2 \times 1.5\ Et_2O$, **6**, **6***, $Mg[\mathbf{7}]_2 \times 2\ C_6H_6$, **8**$\times 0.5\ C_6H_6$, **9**, $(2\text{-}Br\text{-}C_6H_4)Ph_2P \cdot B(H)(C_6F_5)_2 \times 0.5$ toluene, $(Li[\mathbf{13}])_2$, 1,2-$C_6H_4(P(O)t\text{-}Bu_2)(I)$, and 1,2-$C_6H_4(Pt\text{-}Bu_2)(Br)$ were scaled using the frame scaling procedure in the *X-AREA* program system.[S2] All structures were solved by direct methods (program *SHELXS*)[S3] and refined against F^2 with full-matrix least-squares techniques (program *SHELXL-97*)[S3].

In $(Li[\mathbf{2a}])_2$, two *tert*-butyl groups are disordered over two sites with a site occupation factor of 0.57(1) and 0.54(1), respectively, for the major occupied site. Bond lengths and angles in the *tert*-butyl groups were restrained to be equal. The bond C5-C52' was restrained to 1.50(1) Å. The disordered atoms were isotropically refined.

In $(Li[\mathbf{3}])_2$, one t*ert*-butyl group is disordered over two sites with a site occupation factor of 0.61(1) for the major occupied site. The disordered atoms were isotropically refined.

In $Mg(Et_2O)[\mathbf{5}]_2 \times 1.5\ Et_2O$, two C atoms of a co-crystallized Et_2O molecule are disordered over two equally occupied sites.

In $(2\text{-}Br\text{-}C_6H_4)Ph_2P \cdot B(H)(C_6F_5)_2 \times 0.5$ toluene, the H atoms of the methyl group of the toluene molecule are disordered over two equally occupied sites.

The H atoms bonded to B in $(Li[\mathbf{3}])_2$, $(Li[\mathbf{3}])_2 \times C_6H_6$, **4**, $Mg(Et_2O)[\mathbf{5}]_2 \times Et_2O$, $Mg(Et_2O)[\mathbf{5}]_2 \times 1.5\ Et_2O$, **6**, $Mg[\mathbf{7}]_2 \times 2\ C_6H_6$, **9**, **12**, $(2\text{-}Br\text{-}C_6H_4)Ph_2P \cdot B(H)(C_6F_5)_2 \times 0.5$ toluene, and $(Li[\mathbf{13}])_2$ were isotropically refined.

The coordinates of the H atom bonded to B in **6*** were refined.

S1. Spek, A. L. *J. Appl. Crystallogr.* **2003**, *36*, 7–13.

S2. *X-AREA. Diffractometer control program system*; Stoe & Cie: Darmstadt, Germany, 2002.

S3. Sheldrick, G. M. *Acta. Crystallogr.* **2008**, *A64*, 112–122.

CCDC reference numbers: CCDC 994607 ((Li[**2a**])$_2$), 994608 ((Li[**3**])$_2$×C_6H_6), 994609 ((Li[**3**])$_2$), 994610 (**4**), 994611 (Mg(Et_2O)[**5**]$_2$×Et_2O), 994612 (Mg(Et_2O)[**5**]$_2$×1.5 Et_2O), 994613 (**6**), 994614 (**6***), 994615 (Mg[**7**]$_2$×2 C_6H_6), 994616 (**8**×0.5 C_6H_6), 994617 (**9**), 994606 (**12**), 994618 ((2-Br-C_6H_4)Ph_2P·B(H)(C_6F_5)$_2$×0.5 toluene), 994619 ((Li[**13**])$_2$), 994620 (1,2-C_6H_4(P(O)*t*-Bu_2)(I)), and 994621 (1,2-C_6H_4(P*t*-Bu_2)(Br)).

Li[**2a**] was synthesized as described in the one-pot synthesis of **4** in the main paper. Instead of adding $Li[AlH_4]$, all volatiles were removed under vacuum, pentane (20 mL) was added, and the resulting mixture was filtered. After the filter cake had been washed with pentane (10 mL), the filtrate was concentrated until it turned slightly turbid and stored at −40 °C, whereupon colorless plate-shaped crystals of $(Li[\mathbf{2a}])_2$ formed.

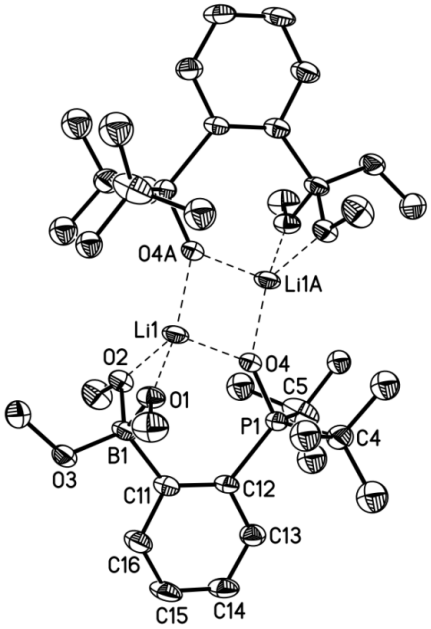

Figure S11. Solid-state structure of $(Li[\mathbf{2a}])_2$ (monoclinic, $P2_1/c$). Displacement ellipsoids are drawn at the 50% probability level. Hydrogen atoms are omitted for clarity. Selected bond lengths [Å], bond angles [deg], and torsion angle [deg]: Li(1)–O(1) = 1.888(6), Li(1)–O(2) = 1.871(6), Li(1)–O(4) = 1.904(6), Li(1)–O(4A) = 1.902(6), B(1)–O(1) = 1.481(4), B(1)–O(2) = 1.485(5), B(1)–O(3) = 1.452(4), B(1)–C(11) = 1.646(5), P(1)–O(4) = 1.504(2), P(1)–C(12) = 1.828(3), C(11)–C(12) = 1.422(5); Li(1)–O(4)–Li(1A) = 81.3(3), B(1)–C(11)–C(12) = 129.3(3), O(1)–B(1)–O(2) = 99.4(2), O(1)–Li(1)–O(2) = 74.0(2), O(4)–Li(1)–O(4A) = 98.7(3), P(1)–C(12)–C(11) = 127.3(2), P(1)–O(4)–Li(1) = 136.2(2); B(1)–C(11)–C(12)–P(1) = 1.3(5). Symmetry transformation used to generate equivalent atoms A: –x, –y+1, –z+1.

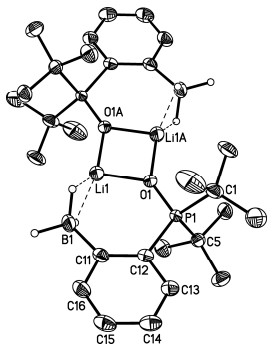

Figure S12. Solid-state structure of $(Li[\mathbf{3}])_2 \times C_6H_6$ (monoclinic, $P2_1/c$). Displacement ellipsoids are drawn at the 50% probability level. Hydrogen atoms (except on boron) and co-crystallized C_6H_6 are omitted for clarity. Selected bond lengths [Å], atom···atom distance [Å], bond angles [deg], and torsion angle [deg]: B(1)···Li(1) = 2.226(3), B(1)–C(11) = 1.623(3), P(1)–C(12) = 1.821(2), P(1)–O(1) = 1.518(2), O(1)–Li(1) = 1.852(3), O(1)–Li(1A) = 1.869(3), C(11)–C(12) = 1.415(2); B(1)–C(11)–C(12) = 129.0(2), O(1)–P(1)–C(12) = 113.6(1), O(1)–Li(1)–O(1A) = 96.5(2), P(1)–C(12)–C(11) = 124.5(2), Li(1)–O(1)–Li(1A) = 83.5(2); B(1)–C(11)–C(12)–P(1) = 5.2(2). Symmetry transformation used to generate equivalent atoms A: –x+1, –y+1, –z+1.

Colorless block-shaped crystals of $(Li[\mathbf{3}])_2$, a pseudo-polymorph of $(Li[\mathbf{3}])_2 \times C_6H_6$, were obtained by slow evaporation of a solution of Li[**3**] in Et_2O (cf. Figure S9).

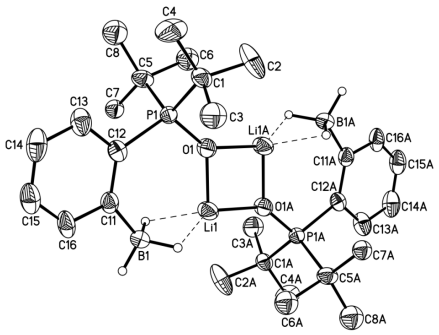

Figure S13. Solid-state structure of $(Li[\mathbf{3}])_2$ (monoclinic, $P2_1/c$). Displacement ellipsoids are drawn at the 30% probability level. Hydrogen atoms (except on boron) are omitted for clarity. Selected bond lengths [Å], atom···atom distance [Å], bond angles [deg], and torsion angle [deg]: B(1)···Li(1) = 2.206(8), B(1)–C(11) = 1.602(6), P(1)–C(12) = 1.818(3), P(1)–O(1) = 1.524(2), O(1)–Li(1) = 1.863(7), O(1)–Li(1A) = 1.851(7), C(11)–C(12) = 1.397(5); B(1)–C(11)–C(12) = 129.6(3), O(1)–P(1)–C(12) = 111.5(2), O(1)–Li(1)–O(1A) = 97.8(3), P(1)–C(12)–C(11) = 126.6(3), Li(1)–O(1)–Li(1A) = 82.2(3); B(1)–C(11)–C(12)–P(1) = –4.5(6). Symmetry transformation used to generate equivalent atoms A: –x+1, –y+1, –z+1.

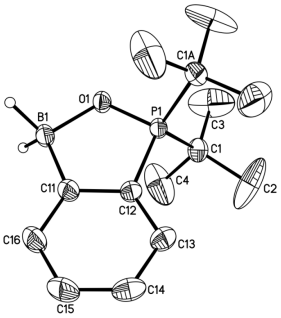

Figure S14. Solid-state structure of **4** (orthorhombic, *Pnma*). Displacement ellipsoids are drawn at the 50% probability level. Hydrogen atoms (except on boron) are omitted for clarity. Selected bond lengths [Å], bond angles [deg], and torsion angle [deg]: B(1)–C(11) = 1.607(4), B(1)–O(1) = 1.584(3), P(1)–C(12) = 1.781(2), P(1)–O(1) = 1.542(2), C(11)–C(12) = 1.399(3); B(1)–O(1)–P(1) = 114.2(2), B(1)–C(11)–C(12) = 115.1(2), O(1)–B(1)–C(11) = 102.7(2), O(1)–P(1)–C(12) = 100.7(1), P(1)–C(12)–C(11) = 107.4(2); B(1)–C(11)–C(12)–P(1) = 0. Symmetry transformation used to generate equivalent atoms A: x, –y+3/2, z.

A solution of **4** (0.12 g, 0.48 mmol) in Et_2O (10 mL) was added to freshly prepared C_6F_5MgBr (0.51 mmol) in Et_2O (5 mL) at room temperature. Filtration and removal of all volatiles from the filtrate under vacuum yielded crude Mg[**5**]$_2$. The material was redissolved in Et_2O and the solution was stored at ambient temperature to grow colorless block-shaped crystals of Mg(Et_2O)[**5**]$_2$×1.5 Et_2O suitable for X-ray crystallography (cf. Figure S12). The mother liquor was slowly evaporated on air, whereupon crystals of the pseudo-polymorph Mg(Et_2O)[**5**]$_2$×Et_2O formed (cf. Figure S11).

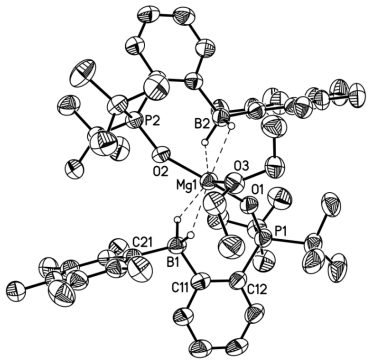

Figure S15. Solid-state structure of $Mg(Et_2O)[\mathbf{5}]_2\times Et_2O$ (orthorhombic, *Pbcn*). Displacement ellipsoids are drawn at the 50% probability level. Hydrogen atoms (except on boron) and co-crystallized Et_2O are omitted for clarity. Selected bond lengths [Å], atom···atom distances [Å], bond angles [deg], and torsion angle [deg]: B(1)···Mg(1) = 2.555(4), B(1)–C(11) = 1.629(5), B(1)–C(21) = 1.622(5), B(2)···Mg(1) = 2.550(4), B(2)–C(51) = 1.619(5), B(2)–C(61) = 1.629(5), P(1)–C(12) = 1.804(3), P(1)–O(1) = 1.513(2), P(2)–O(2) = 1.515(2), O(1)–Mg(1) = 1.957(2), O(2)–Mg(1) = 1.951(2), O(3)–Mg(1) = 2.087(2), C(11)–C(12) = 1.424(4); B(1)–Mg(1)–B(2) = 143.1(2), B(1)–Mg(1)–O(2) = 95.1(2), B(1)–C(11)–C(12) = 126.2(3), O(1)–P(1)–C(12) = 113.3(2), O(1)–Mg(1)–O(2) = 164.4(2), P(1)–C(12)–C(11) = 123.0(2); B(1)–C(11)–C(12)–P(1) = –9.5(5).

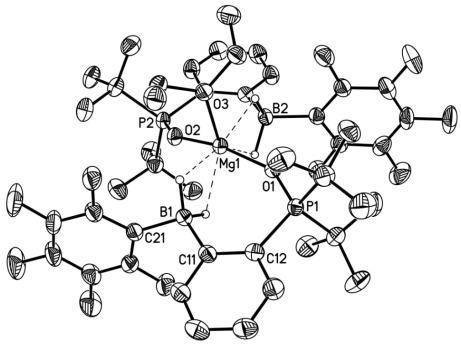

Figure S16. Solid-state structure of $Mg(Et_2O)[\mathbf{5}]_2\times 1.5\ Et_2O$ (orthorhombic, *Pbcn*). Displacement ellipsoids are drawn at the 50% probability level. Hydrogen atoms (except on boron) and co-crystallized Et_2O are omitted for clarity. Selected bond lengths [Å], atom···atom distances [Å], bond angles [deg], and torsion angle [deg]: B(1)···Mg(1) = 2.520(3), B(1)–C(11) = 1.629(4), B(1)–C(21) = 1.621(3), B(2)···Mg(1) = 2.524(3), P(1)–C(12) = 1.814(2), P(1)–O(1) = 1.505(2), O(1)–Mg(1) = 1.960(2), O(2)–Mg(1) = 1.958(2), O(3)–Mg(1) = 2.099(2), C(11)–C(12) = 1.415(3); B(1)–Mg(1)–B(2) = 143.4(1), B(1)–Mg(1)–O(2) = 93.2(1), B(1)–C(11)–C(12) = 126.2(2), O(1)–P(1)–C(12) = 113.4(1), O(1)–Mg(1)–O(2) = 164.3(1), P(1)–C(12)–C(11) = 123.7(2); B(1)–C(11)–C(12)–P(1) = –1.3(4).

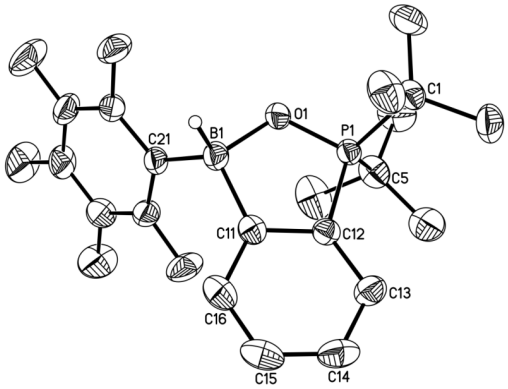

Figure S17. Solid-state structure of **6** (monoclinic, $P2_1/c$). Displacement ellipsoids are drawn at the 50% probability level. Hydrogen atoms (except on boron) are omitted for clarity. Selected bond lengths [Å], bond angles [deg], and torsion angle [deg]: B(1)–C(11) = 1.604(2), B(1)–C(21) = 1.634(2), B(1)–O(1) = 1.574(2), P(1)–C(12) = 1.785(2), P(1)–O(1) = 1.545(2), C(11)–C(12) = 1.401(2); B(1)–O(1)–P(1) = 114.4(1), B(1)–C(11)–C(12) = 114.6(2), O(1)–B(1)–C(11) = 102.9(2), O(1)–P(1)–C(12) = 100.1(1), P(1)–C(12)–C(11) = 107.5(2); B(1)–C(11)–C(12)–P(1) = –5.4(2).

Colorless plate-shaped crystals of a polymorph **6*** of **6** were obtained by slow evaporation of a solution of **6** in C_6H_6 (cf. Figure S14).

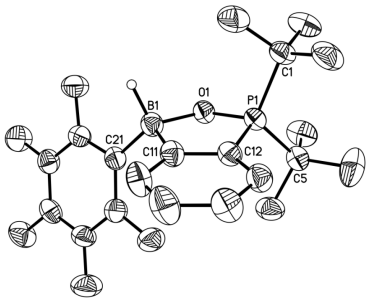

Figure S18. Solid-state structure of **6*** (monoclinic, $P2_1/n$). Displacement ellipsoids are drawn at the 50% probability level. Hydrogen atoms (except on boron) are omitted for clarity. Selected bond lengths [Å], bond angles [deg], and torsion angle [deg]: B(1)–C(11) = 1.617(3), B(1)–C(21) = 1.633(3), B(1)–O(1) = 1.566(3), P(1)–C(12) = 1.785(2), P(1)–O(1) = 1.550(2), C(11)–C(12) = 1.398(3); B(1)–O(1)–P(1) = 114.1(2), B(1)–C(11)–C(12) = 114.9(2), O(1)–B(1)–C(11) = 102.5(2), O(1)–P(1)–C(12) = 100.2(1), P(1)–C(12)–C(11) = 107.1(2); B(1)–C(11)–C(12)–P(1) = 0.7(2).

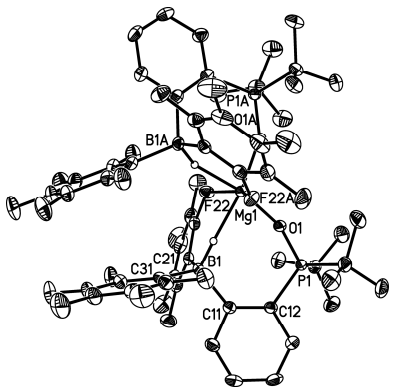

Figure S19. Solid-state structure of Mg[**7**]$_2$×2 C_6H_6 (monoclinic, *C*2/*c*). Displacement ellipsoids are drawn at the 50% probability level. Hydrogen atoms (except on boron) and co-crystallized C_6H_6 are omitted for clarity. Selected bond lengths [Å], atom···atom distance [Å], bond angles [deg], and torsion angle [deg]: B(1)···Mg(1) = 3.002(2), B(1)–C(11) = 1.645(2), B(1)–C(21) = 1.640(2), B(1)–C(31) = 1.639(2), P(1)–C(12) = 1.814(2), P(1)–O(1) = 1.512(1), O(1)–Mg(1) = 1.892(2), F(22)–Mg(1) = 2.075(1), C(11)–C(12) = 1.416(2); B(1)–Mg(1)–O(1) = 76.4(1), B(1)–C(11)–C(12) = 128.8(2), O(1)–P(1)–C(12) = 113.2(1), O(1)–Mg(1)–F(22) = 95.9(1), P(1)–C(12)–C(11) = 126.6(2); B(1)–C(11)–C(12)–P(1) = 2.3(2). Symmetry transformation used to generate equivalent atoms A: –x+1, y, –z+1/2.

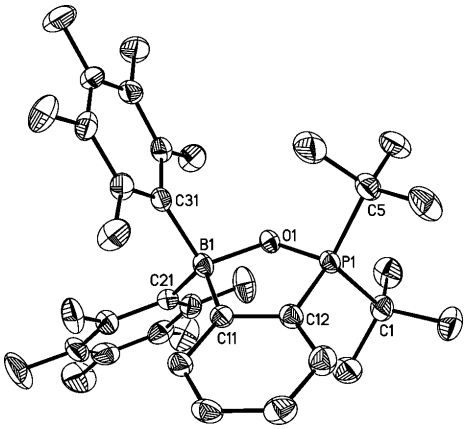

Figure S20. Solid-state structure of **8**×0.5 C_6H_6 (triclinic, *P*–1). Displacement ellipsoids are drawn at the 50% probability level. Hydrogen atoms and co-crystallized C_6H_6 are omitted for clarity. Selected bond lengths [Å], bond angles [deg], and torsion angle [deg]: B(1)–C(11) = 1.632(3), B(1)–C(21) = 1.644(3), B(1)–C(31) = 1.646(3), B(1)–O(1) = 1.550(2), P(1)–C(12) = 1.780(2), P(1)–O(1) = 1.546(2), C(11)–C(12) = 1.402(3); B(1)–O(1)–P(1) = 115.9(2), B(1)–C(11)–C(12) = 113.6(2), O(1)–B(1)–C(11) = 102.3(2), O(1)–P(1)–C(12) = 99.4(1), P(1)–C(12)–C(11) = 108.3(2); B(1)–C(11)–C(12)–P(1) = –3.7(2).

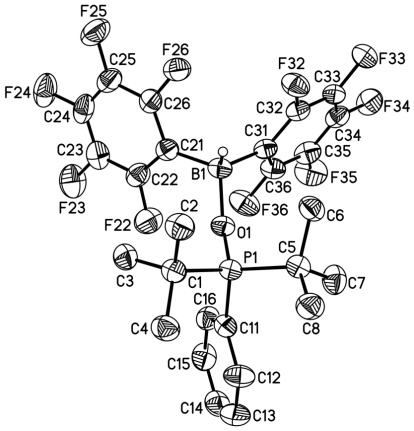

Figure S21. Compound **9** crystallizes with two independent molecules (**9**$^{\mathbf{A}}$ and **9**$^{\mathbf{B}}$) in the asymmetric unit. Even though the conformations of **9**$^{\mathbf{A}}$ and **9**$^{\mathbf{B}}$ are different, all key bond lengths and angles are the same within the experimental error margins. Thus, only the solid-state structure of **9**$^{\mathbf{A}}$ (triclinic, *P*–1) is shown above. Displacement ellipsoids are drawn at the 50% probability level. Hydrogen atoms (except on boron) are omitted for clarity. Selected bond lengths [Å], bond angles [deg], and torsion angle [deg]: B(1)–C(21) = 1.635(4), B(1)–C(31) = 1.636(3), B(1)–O(1) = 1.524(3), P(1)–C(1) = 1.855(2), P(1)–C(5) = 1.845(2), P(1)–C(11) = 1.799(2), P(1)–O(1) = 1.531(2); B(1)–O(1)–P(1) = 138.4(2), O(1)–B(1)–C(21) = 111.8(2), O(1)–B(1)–C(31) = 108.3(2), O(1)–P(1)–C(11) = 103.6(1), C(1)–P(1)–C(5) = 115.7(2); B(1)–O(1)–P(1)–C(11) = 177.9(2).

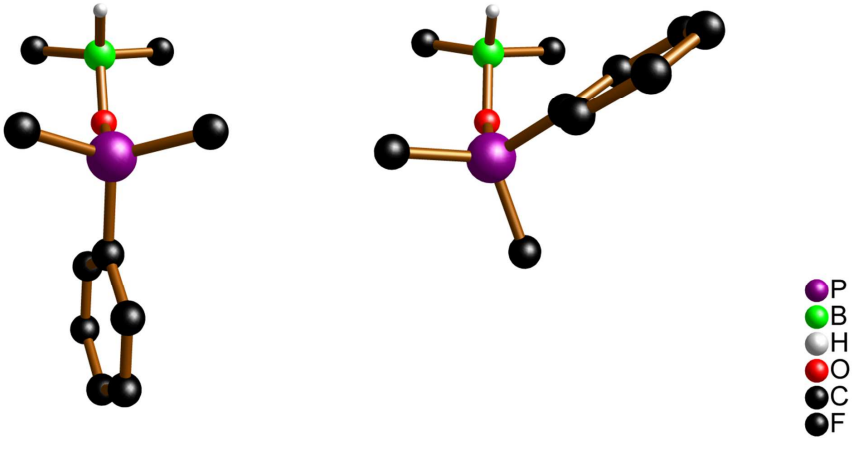

Figure S22. Comparison of the molecular conformations of **9**$^{\mathbf{A}}$ and **9**$^{\mathbf{B}}$ in the solid state. Hydrogen atoms (except on boron) and the carbon atoms of the methyl groups are omitted for clarity; only the *ipso*-carbon atoms of the C_6F_5 rings are shown.

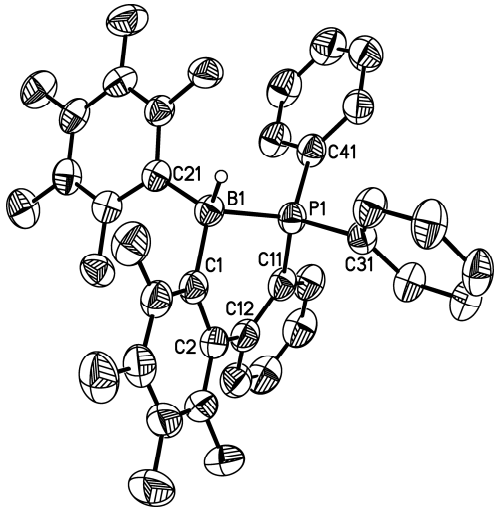

Figure S23. Solid-state structure of **12** (monoclinic, $P2_1/n$). Displacement ellipsoids are drawn at the 50% probability level. Hydrogen atoms (except on boron) are omitted for clarity. Selected bond lengths [Å], bond angles [deg], and torsion angles [deg]: B(1)–P(1) = 1.951(2), B(1)–C(1) = 1.617(3), B(1)–C(21) = 1.619(3), P(1)–C(11) = 1.796(2), P(1)–C(31) = 1.812(2), C(2)–C(12) = 1.498(3); B(1)–C(1)–C(2) = 125.3(2), B(1)–P(1)–C(11) = 105.9(1), P(1)–C(11)–C(12) = 118.0(2), P(1)–B(1)–C(1) = 103.2(2); C(1)–B(1)–P(1)–C(11) = 46.0(2), C(1)–C(2)–C(12)–C(11) = 30.3(3).

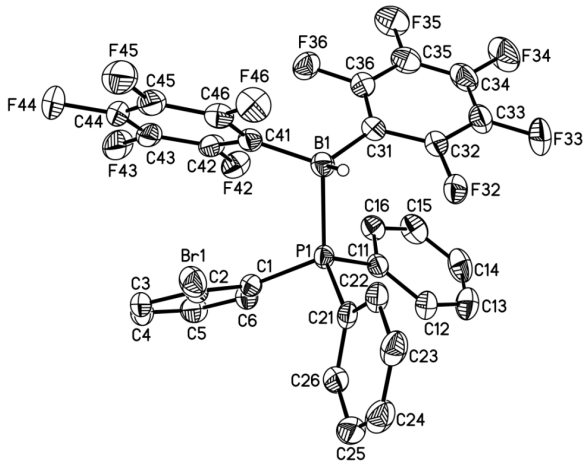

Figure S24. Solid-state structure of (2-Br-C_6H_4)$Ph_2P\cdot B(H)(C_6F_5)_2\times 0.5$ toluene (monoclinic, $C2/c$). Displacement ellipsoids are drawn at the 50% probability level. Hydrogen atoms (except on boron) and co-crystallized toluene are omitted for clarity. Selected bond lengths [Å], bond angles [deg], and torsion angle [deg]: B(1)–P(1) = 2.053(3), B(1)–C(31) = 1.616(4), B(1)–C(41) = 1.614(4), P(1)–C(1) = 1.830(3), P(1)–C(11) = 1.812(3), P(1)–C(21) = 1.811(3); C(1)–P(1)–C(11) = 106.7(2), C(1)–P(1)–C(21) = 104.2(2), C(1)–P(1)–B(1) = 114.9(2), C(31)–B(1)–C(41) = 119.7(2); C(1)–B(1)–P(1)–C(41) = 9.1(2).

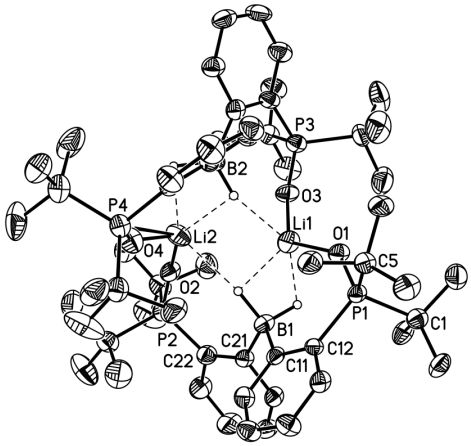

Figure S25. Solid-state structure of (Li[**13**])$_2$ (triclinic, *P*–1). Displacement ellipsoids are drawn at the 50% probability level. Hydrogen atoms (except on boron) are omitted for clarity. Selected bond lengths [Å], atom···atom distances [Å], torsion angles [deg], and dihedral angle [deg]: B(1)···Li(1) = 2.378(11), B(1)···Li(2) = 3.435(11), B(2)···Li(2) = 2.429(11), B(2)···Li(1) = 3.223(11), P(1)–O(1) = 1.498(3), P(2)–O(2) = 1.485(4), P(3)–O(3) = 1.490(4), P(4)–O(4) = 1.493(4), O(1)–Li(1) = 1.839(8), O(2)–Li(2) = 1.826(9), O(3)–Li(1) = 1.841(9), O(4)–Li(2) = 1.809(10); B(1)–C(11)–C(12)–P(1) = 2.2(7), B(1)–C(21)–C(22)–P(2) = –6.1(9); ph(C(11)//ph(C(21) = 52.7(7); ph(C(X)): phenylene ring containing carbon atom X.

Colorless needle-shaped crystals of 1,2-C_6H_4(P(O)*t*-Bu_2)(I) were obtained by storing a concentrated solution of 1,2-C_6H_4(P(O)*t*-Bu_2)(I) in hexane at 6 °C (cf. Figure S22).

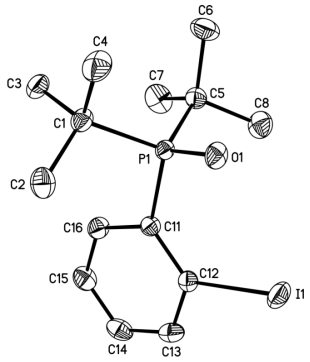

Figure S26. Solid-state structure of 1,2-C_6H_4(P(O)*t*-Bu_2)(I) (monoclinic, $P2_1/n$). Displacement ellipsoids are drawn at the 50% probability level. Hydrogen atoms are omitted for clarity. Selected bond lengths [Å], bond angles [deg], and torsion angle [deg]: I(1)–C(12) = 2.109(2), P(1)–O(1) = 1.484(2), P(1)–C(1) = 1.870(2), P(1)–C(5) = 1.858(2), P(1)–C(11) = 1.829(2), C(11)–C(12) = 1.400(3); I(1)–C(12)–C(11) = 125.5(2), O(1)–P(1)–C(11) = 112.5(1), P(1)–C(11)–C(12) = 125.9(2); I(1)–C(12)–C(11)–P(1) = –2.7(3).

Colorless block-shaped crystals of 1,2-C_6H_4(P*t*-Bu_2)(Br) were obtained by slow evaporation of a solution of 1,2-C_6H_4(P*t*-Bu_2)(Br) in C_6H_6 (cf. Figure S23).

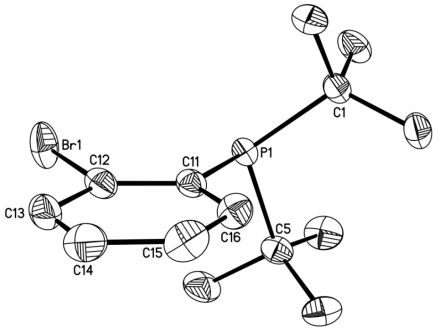

Figure S27. Solid-state structure of 1,2-C_6H_4(P*t*-Bu_2)(Br) (monoclinic, $P2_1/n$). Displacement ellipsoids are drawn at the 50% probability level. Hydrogen atoms are omitted for clarity. Selected bond lengths [Å], bond angles [deg], and torsion angle [deg]: Br(1)–C(12) = 1.907(2), P(1)–C(1) = 1.898(2), P(1)–C(5) = 1.892(2), P(1)–C(11) = 1.852(2), C(11)–C(12) = 1.395(3); Br(1)–C(12)–C(11) = 121.4(2), P(1)–C(11)–C(12) = 120.5(2); Br(1)–C(12)–C(11)–P(1) = –3.6(2).

Table S1. Selected Crystallographic Data for (Li[**2a**])$_2$, (Li[**3**])$_2$×C_6H_6, (Li[**3**])$_2$, and **4**.

	(Li[**2a**])$_2$	(Li[**3**])$_2$×C_6H_6	(Li[**3**])$_2$	**4**
formula	$C_{34}H_{62}B_2Li_2O_8P_2$	$C_{28}H_{50}B_2Li_2O_2P_2$ × C_6H_6	$C_{28}H_{50}B_2Li_2O_2P_2$	$C_{14}H_{24}BOP$
M_r	696.28	594.23	516.12	250.11
color, shape	colorless, plate	colorless, rod	colorless, block	colorless, block
T [K]	173(2)	173(2)	173(2)	173(2)
radiation, λ [Å]	MoKα, 0.71073	MoKα, 0.71073	MoKα, 0.71073	MoKα, 0.71073
crystal system	monoclinic	monoclinic	monoclinic	orthorhombic
space group	$P2_1/c$	$P2_1/c$	$P2_1/c$	*Pnma*
a [Å]	11.6441(14)	8.1751(5)	7.9836(4)	12.6396(7)
b [Å]	11.3912(8)	14.6574(9)	23.4684(12)	11.9670(7)
c [Å]	15.7074(18)	15.4393(9)	8.7674(5)	9.9335(6)
α [°]	90	90	90	90
β [°]	100.691(9)	105.119(5)	107.429(4)	90
γ [°]	90	90	90	90
V [Å^3]	2047.3(4)	1785.99(19)	1567.26(14)	1502.52(15)
Z	2	2	2	4
D_{calcd} [g cm^{-3}]	1.129	1.105	1.094	1.106
F(000)	752	644	560	544
μ· [mm^{-1}]	0.149	0.149	0.160	0.166
crystal size [mm]	0.36 × 0.22 × 0.13	0.49 × 0.23 × 0.16	0.52 × 0.49 × 0.49	0.50 × 0.20 × 0.15
rflns collected	22338	19463	20941	22041
independent rflns (R_{int})	3848 (0.0998)	3345 (0.0795)	2752 (0.0698)	1820 (0.0790)
data/restraints/parameters	3848/133/213	3345/0/202	2752/0/173	1820/0/95
GOF on F^2	1.095	1.063	1.065	1.149
R_1, wR_2 [$I > 2\sigma(I)$]	0.0646, 0.1573	0.0408, 0.1038	0.0836, 0.2157	0.0523, 0.1297
R_1, wR_2 (all data)	0.0801, 0.1654	0.0450, 0.1064	0.0854, 0.2170	0.0566, 0.1326
largest diff peak and hole [e Å^{-3}]	0.641, −0.485	0.409, −0.245	0.720, −0.466	0.328, −0.326

Table S2. Selected Crystallographic Data for $Mg(Et_2O)[\mathbf{5}]_2\times Et_2O$, $Mg(Et_2O)[\mathbf{5}]_2\times 1.5\ Et_2O$, **6**, and **6***.

	$Mg(Et_2O)[\mathbf{5}]_2\times Et_2O$	$Mg(Et_2O)[\mathbf{5}]_2\times 1.5\ Et_2O$	**6**	**6***
formula	$C_{44}H_{58}B_2F_{10}MgO_3P_2 \times Et_2O$	$C_{44}H_{58}B_2F_{10}MgO_3P_2 \times 1.5\ Et_2O$	$C_{20}H_{23}BF_5OP$	$C_{20}H_{23}BF_5OP$
M_r	1006.89	1043.95	416.16	416.16
color, shape	colorless, plate	colorless, block	colorless, block	colorless, plate
T [K]	173(2)	173(2)	173(2)	173(2)
radiation, λ [Å]	MoKα, 0.71073	MoKα, 0.71073	MoKα, 0.71073	MoKα, 0.71073
crystal system	orthorhombic	orthorhombic	monoclinic	monoclinic
space group	*Pbcn*	*Pbcn*	$P2_1/c$	$P2_1/n$
a [Å]	24.9163(11)	26.1843(8)	8.2095(5)	8.2394(6)
b [Å]	18.1628(6)	17.9091(4)	20.6490(9)	12.3234(9)
c [Å]	23.2274(8)	23.3892(6)	12.0842(7)	19.8146(17)
α [°]	90	90	90	90
β [°]	90	90	100.620(5)	91.291(6)
γ [°]	90	90	90	90
V [Å^3]	10511.6(7)	10968.1(5)	2013.40(19)	2011.4(3)
Z	8	8	4	4
D_{calcd} [g cm^{-3}]	1.272	1.264	1.373	1.374
F(000)	4240	4408	864	864
$\mu\cdot$ [mm^{-1}]	0.170	0.166	0.189	0.189
crystal size [mm]	0.58 × 0.14 × 0.05	0.56 × 0.32 × 0.22	0.25 × 0.20 × 0.15	0.39 × 0.10 × 0.04
rflns collected	71628	127963	25742	20133
independent rflns (R_{int})	9596 (0.1167)	10128 (0.1085)	4205 (0.0625)	3553 (0.1190)
data/restraints/parameters	9596/0/620	10128/0/653	4205/0/257	3553/0/256
GOF on F^2	1.016	1.079	1.087	1.042
R_1, wR_2 [$I > 2\sigma(I)$]	0.0628, 0.1123	0.0542, 0.1179	0.0419, 0.1043	0.0485, 0.1240
R_1, wR_2 (all data)	0.1189, 0.1319	0.0791, 0.1274	0.0485, 0.1080	0.0639, 0.1328
largest diff peak and hole [e Å^{-3}]	0.274, −0.266	0.302, −0.298	0.268, −0.264	0.323, −0.265

Table S3. Selected Crystallographic Data for Mg[**7**]$_2$×2 C_6H_6, **8**×0.5 C_6H_6, **9**, and **12**.

	Mg[**7**]$_2$×2 C_6H_6	**8**×0.5 C_6H_6	**9**	**12**
formula	$C_{52}H_{46}B_2F_{20}MgO_2P_2$ × 2 C_6H_6	$C_{26}H_{22}BF_{10}OP$ × 0.5 C_6H_6	$C_{26}H_{24}BF_{10}OP$	$C_{30}H_{15}BF_9P$
M_r	1346.97	621.27	584.23	588.20
color, shape	colorless, block	colorless, block	colorless, rod	colorless, block
T [K]	173(2)	173(2)	173(2)	173(2)
radiation, λ [Å]	MoKα, 0.71073	MoKα, 0.71073	MoKα, 0.71073	MoKα, 0.71073
crystal system	monoclinic	triclinic	triclinic	monoclinic
space group	*C*2/*c*	*P*–1	*P*–1	$P2_1/n$
a [Å]	21.5498(8)	10.5698(9)	11.7547(8)	10.1228(5)
b [Å]	13.5816(7)	12.2356(10)	15.4233(10)	20.2441(7)
c [Å]	22.3381(9)	12.7246(11)	15.8242(11)	13.1500(5)
α [°]	90	111.819(6)	102.286(5)	90
β [°]	110.854(3)	97.953(7)	92.657(5)	109.605(3)
γ [°]	90	110.112(6)	110.511(5)	90
V [Å^3]	6109.6(5)	1366.1(2)	2602.4(3)	2538.57(18)
Z	4	2	4	4
D_{calcd} [g cm^{-3}]	1.464	1.510	1.491	1.539
F(000)	2760	634	1192	1184
μ· [mm^{-1}]	0.188	0.192	0.196	0.195
crystal size [mm]	0.16 × 0.16 × 0.10	0.04 × 0.03 × 0.02	0.10 × 0.03 × 0.03	0.35 × 0.32 × 0.27
rflns collected	43010	29118	42651	30875
independent rflns (R_{int})	5605 (0.0574)	5114 (0.0843)	10038 (0.0653)	4939 (0.0496)
data/restraints/parameters	5605/0/416	5114/0/379	10038/0/711	4939/0/374
GOF on F^2	1.065	1.002	0.980	1.035
R_1, wR_2 [$I > 2\sigma(I)$]	0.0343, 0.0856	0.0433, 0.0890	0.0448, 0.0936	0.0397, 0.1035
R_1, wR_2 (all data)	0.0375, 0.0875	0.0687, 0.0968	0.0764, 0.1041	0.0500, 0.1089
largest diff peak and hole [e Å^{-3}]	0.331, −0.295	0.282, −0.276	0.290, −0.395	0.282, −0.212

Table S4. Selected Crystallographic Data for (2-Br-C_6H_4)$Ph_2P\cdot B(H)(C_6F_5)_2\times$0.5 toluene, (Li[**13**])$_2$, 1,2-C_6H_4(P(O)*t*-Bu_2)(I), and 1,2-C_6H_4(P*t*-Bu_2)(Br).

	(2-Br-C_6H_4)$Ph_2P\cdot B(H)(C_6F_5)_2$ ×0.5 toluene	(Li[**13**])$_2$	1,2-C_6H_4(P(O)*t*-Bu_2)(I)	1,2-C_6H_4(P*t*-Bu_2)(Br)
formula	$C_{30}H_{15}BBrF_{10}P$ × 0.5 toluene	$C_{112}H_{184}B_4Li_4O_8P_8$	$C_{14}H_{22}IOP$	$C_{14}H_{22}BrP$
M_r	733.18	1977.34	364.19	301.19
color, shape	colorless, plate	colorless, block	colorless, needle	colorless, block
T [K]	173(2)	173(2)	173(2)	173(2)
radiation, λ [Å]	MoKα, 0.71073	MoKα, 0.71073	MoKα, 0.71073	MoKα, 0.71073
crystal system	monoclinic	triclinic	monoclinic	monoclinic
space group	*C*2/*c*	*P*–1	$P2_1/n$	$P2_1/n$
a [Å]	42.451(3)	11.822(2)	9.7229(7)	9.7908(12)
b [Å]	8.0922(5)	13.840(2)	15.4677(8)	15.5575(16)
c [Å]	18.3949(10)	19.008(3)	10.4030(7)	10.0203(12)
α [°]	90	77.506(12)	90	90
β [°]	111.974(4)	87.659(14)	101.580(6)	104.322(9)
γ [°]	90	76.638(12)	90	90
V [Å^3]	5860.0(6)	2954.0(8)	1532.67(17)	1478.9(3)
Z	8	1	4	4
D_{calcd} [g cm^{-3}]	1.662	1.112	1.578	1.353
F(000)	2920	1072	728	624
$\mu\cdot$ [mm^{-1}]	1.547	0.169	2.178	2.863
crystal size [mm]	0.21 × 0.13 × 0.08	0.11 × 0.05 × 0.02	0.50 × 0.05 × 0.05	0.25 × 0.25 × 0.19
rflns collected	45650	24064	22472	8397
independent rflns (R_{int})	5367 (0.0739)	10380 (0.1538)	3122 (0.0931)	2764 (0.0572)
data/restraints/parameters	5367/0/425	10380/0/629	3122/0/154	2764/0/145
GOF on F^2	1.048	0.730	1.068	1.029
R_1, wR_2 [$I > 2\sigma(I)$]	0.0418, 0.1014	0.0629, 0.0939	0.0236, 0.0605	0.0315, 0.0760
R_1, wR_2 (all data)	0.0516, 0.1065	0.1862, 0.1308	0.0259, 0.0615	0.0390, 0.0789
largest diff peak and hole [e Å^{-3}]	0.454, −0.489	0.231, −0.275	0.448, −0.591	0.437, −0.762